

## Accepted Manuscript

Title: Dye-Based Photonic Sensing Systems

Author: <ce:author id="aut0005" biographyid="vt0005" orcid="0000-0003-2010-1223"> Francisco J. Aparicio María Alcaire Agustín R. González-Elipe Angel Barranco Miguel Holgado Rafael Casquel Francisco J. Sanza Amadeu Griol Damien Bernier Fabian Dortu Santiago Cáceres Mikael Antelius Martin Lapisa<ce:author id="aut0070" biographyid="vt0070" orcid="0000-0002-2650-0121"> Hans Sohlström Frank Niklaus



PII: S0925-4005(16)30092-2  
DOI: <http://dx.doi.org/doi:10.1016/j.snb.2016.01.092>  
Reference: SNB 19601

To appear in: *Sensors and Actuators B*

Received date: 11-7-2015  
Revised date: 16-1-2016  
Accepted date: 19-1-2016

Please cite this article as: Francisco J.Aparicio, María Alcaire, Agustín R.González-Elipe, Angel Barranco, Miguel Holgado, Rafael Casquel, Francisco J.Sanza, Amadeu Griol, Damien Bernier, Fabian Dortu, Santiago Cáceres, Mikael Antelius, Martin Lapisa, Hans Sohlström, Frank Niklaus, Dye-Based Photonic Sensing Systems, Sensors and Actuators B: Chemical <http://dx.doi.org/10.1016/j.snb.2016.01.092>

This is a PDF file of an unedited manuscript that has been accepted for publication. As a service to our customers we are providing this early version of the manuscript. The manuscript will undergo copyediting, typesetting, and review of the resulting proof before it is published in its final form. Please note that during the production process errors may be discovered which could affect the content, and all legal disclaimers that apply to the journal pertain.

## Dye-Based Photonic Sensing Systems

Francisco J. Aparicio<sup>a</sup>, María Alcaire<sup>a</sup>, Agustín R. González-Elipé<sup>a</sup>, Angel Barranco<sup>a</sup>, Miguel Holgado<sup>b</sup>, Rafael Casquel<sup>b</sup>, Francisco J. Sanza<sup>b1</sup>, Amadeu Griol<sup>d</sup>, Damien Bernier<sup>c</sup>, Fabian Dortu<sup>c</sup>, Santiago Cáceres<sup>f</sup>, Mikael Antelius<sup>g 2</sup>, Martin Lapisas<sup>g3</sup>, Hans Sohlström<sup>g</sup> (corresponding author, [hans.sohlstrom@ee.kth.se](mailto:hans.sohlstrom@ee.kth.se), +4687909041), Frank Niklaus<sup>g</sup>.

<sup>a</sup> Instituto de Ciencia de Materiales de Sevilla (CSIC-Universidad de Sevilla), c/Américo Vespucio 49, 41092, Sevilla, Spain.

<sup>b</sup> Group of Optics, Photonics and Biophotonics Group, Center for Biomedical Technology, Universidad Politécnica de Madrid, Campus Montegancedo, 28223 Pozuelo de Alarcón. Madrid, Spain.

<sup>c</sup> Department of applied physics and material engineering, Escuela Técnica superior de ingenieros Industriales (ETSII), Universidad Politécnica de Madrid, Jose Gutiérrez Abascal 2, 28006 Madrid, Spain.

<sup>d</sup> Centro de Tecnología Nanofotónica, Universitat Politècnica de València, Camino de Vera s/n 46022, Valencia, Spain.

<sup>e</sup> Multitel a.s.b.l., B-7000 Mons, Belgium.

<sup>f</sup> ETRA I+D, Avd. Tres Forques, 46014, Valencia, Spain.

<sup>g</sup> KTH Royal Institute of Technology, Department of Micro and Nanosystems, Osquldas väg 10, 100 44 Stockholm, Sweden.

---

<sup>1</sup> Francisco Javier Sanzas current affiliation is Centre for Biomedical Technology. Universidad Politécnica de Madrid. Campus de Montegancedo. Pozuelo de Alarcón, 28223 Madrid, Spain.

<sup>2</sup> Mikael Antelius current affiliation is APR Technologies AB, Västra Järnvägsgatan 4, 745 39 Enköping, Sweden.

<sup>3</sup> Martin Lapisas current affiliation is Bosch Automotive Electronics, Tuebinger Strasse 123, 72762 Reutlingen, Baden-Wuerttemberg, Germany

## Abstract

We report on dye-based photonic sensing systems which are fabricated and packaged at wafer scale. For the first time luminescent organic nanocomposite thin-films deposited by plasma technology are integrated in photonic sensing systems as active sensing elements. The realized dye-based photonic sensors include an environmental NO<sub>2</sub> sensor and a sunlight ultraviolet light (UV) A+B sensor. The luminescent signal from the nanocomposite thin-films responds to changes in the environment and is selectively filtered by a photonic structure consisting of a Fabry-Perot cavity. The sensors are fabricated and packaged at wafer-scale, which makes the technology viable for volume manufacturing. Prototype photonic sensor systems have been tested in real-world scenarios.

Keywords: photonic sensor; dye thin films; gas sensor; UV sensor; room-temperature wafer level packaging

## 1. Introduction

Optical sensors for environmental monitoring and gas sensing offer a number of attractive features including good sensing capabilities, interference immunity and safety [1]. For example, fibre optical sensors may be used in environments in which the use of electrical sensors is not allowed (e.g. for explosives) [2]. They also allow distributed sensing, but their manufacturing often becomes economically challenging because of its serial nature. In contrast, optical dye-based sensors can potentially be manufactured at low cost at wafer scale. However, previous methods for synthesis of active dye thin-films containing a chromophore molecule have not been well developed [3]. Existing methods for preparation of organic nanostructured dye thin-films and other related nanostructured organic or hybrid materials with photonic functionalities typically are based on wet chemical methods. They are not always straightforward or environmentally friendly. In addition, the integration of optically active dye thin-films with photonic sensing structures is challenging because of the optical coupling requirements and the need for interaction of the dye thin films with the environment. These shortcomings have restricted the development of dye-based optical sensors and limited their viability for high-volume applications.

In this work, new types of luminescent thin-films have been prepared by remote plasma assisted vacuum deposition (RPAVD); a new plasma deposition technique that combines plasma polymerization processes with the remote vacuum sublimation of organic dyes. Very flat thin-films with a high concentration of fluorescent dye molecules can thus be obtained [3–6]. The resulting hybrid thin-films are characterized by well-defined  $n$  and  $k$  values and the preservation of the photonic properties such as the luminescence of the dye molecules. This is in strong contrast to the properties of films deposited using conventional plasma enhanced CVD or polymerization methods, in which all precursor molecules are fragmented, and the obtained thin films do not preserve the structure and functionalities of the starting precursor molecules.

In the sensor systems presented in this work, the dye thin-films are integrated on top of the photonic structures, consisting of vertical resonant cavities (VCs), tuned to the

characteristic fluorescence wavelength of the dye thin-films. Sensing transduction results from the changes in the luminescence intensity at this wavelength due to the dye thin-film interaction with the medium. For accurate detection, it is essential to achieve good coupling of the dye thin-film to the photonic structure. At the same time, the active parts of the sensor system must be accessible to the sensing medium (e.g. the gas for gas sensors or UV light for UV sensors), while simultaneously being protected against potential harsh environmental influences (e.g. dust, contamination, corrosion, mechanical damage, etc.). Achieving this in an economical way requires wafer scale fabrication and system integration, including a versatile and robust packaging procedure. Sensor packaging is a costly part of the manufacturing process and is crucial for reliability, yet often the package part most likely to fail or negatively influence the system response [7]. Implementing wafer-level packaging can reduce the cost for the complete system and allow very high integration densities. Currently, low temperature wafer-level packaging methods predominately use polymer adhesives such as UV curable resins [8], BCB [9] or polymer underfills [10–12]. However, dye thin-films can be affected when they come into contact with polymers or solvents that are typically used for wafer-level packaging. Additionally, polymers may absorb or react with the analyte gas in gas sensors, making them unsuitable for use inside the sensor compartment where the supply of the analyte may be restricted and analyte scavenging reactions could locally reduce the analyte concentrations. This problem can be overcome by exclusively using non-reactive materials, such as metals, inside the sensor cavities [11–14]. For the dye-based photonic sensors realized here, a room-temperature wafer-scale packaging approach is utilized [15]. The sensor cavity is sealed by a plastically deformable metal gasket in combination with a room-temperature curable epoxy outside the sensor cavity to provide the permanent bond between the parts of the package.

The optical sensing systems for environmental  $\text{NO}_2$  sensing and for sunlight ultraviolet light (UV) A+B sensing described here are the first sensing systems that integrate luminescent thin-film active sensor elements which are formed by dye molecules embedded in a solid plasma polymeric matrix, together with photonic structures. The measurement principle of the sensors is demonstrated by laboratory experiments, and experiments in a real-world setting are reported to illustrate the practical utility of the sensing systems.

## **2. Concept of the dye-based sensor systems**

### **2.1. Transduction principle of the dye-based photonic sensors**

The design of the dye-based photonic sensors relies on vertical resonant cavities acting as selective transducers of the fluorescent emission that is generated by a dye thin-film upon excitation. The working principle is schematically described in Fig. 1. The vertical resonant cavity covers the entire wafer surface, whereas the sensing areas are defined by the selective deposition of dye thin-film on parts of the resonant cavity surface.

In the case of UV radiation sensing (Fig. 1a), the radiation excites the dye thin-film and causes fluorescent emission. The fluorescence is selectively transmitted by the vertical

resonant cavity, which is tuned to the luminescence wavelength. The sensor read-out is performed via the backside of the chip.

For the NO<sub>2</sub> sensor (Fig. 1b), a light source (e.g. a LED) in the platform excites the dye thin-film, which then generates an emission that is correlated to the NO<sub>2</sub> level because of the fluorescence quenching of the dye emission. In contrast to the sunlight excitation, the excitation light from the LED is stable and approximately perpendicular to the sensor chip. This allows a lateral detection arrangement to further reduce the leak-through of the excitation light, which is perpendicular to the film, while the fluorescence light is radiated in all directions. A significant fraction of the fluorescence emission is guided by the glass substrate to the chip edges, where it is detected. This configuration is especially useful for short-Stokes-shift sensing films such as in the NO<sub>2</sub> optical sensor used here, because light from the excitation source that happens to fall within the detection spectral window (mainly the excitation tail and other spurious components in low cost illumination sources) is transmitted through the structure (c.f. Fig. 1b) and will thus not reach the detector. This improves the signal to noise ratio. Optionally the sensor response of the final device can be further enhanced by covering the back-side of the glass substrate with a thin reflective layer.

The vertical resonant cavity designs in the sensing systems shown in Fig. 1 consist of Fabry-Perot resonant cavities adapted to the fluorescence of the dye thin-film materials. The resonant structure incorporates an optical defect in a periodic 1-D photonic crystal creating a photonic bandgap. The defect is equivalent to the cavity in a conventional Fabry-Perot resonator. The cavities are defined by a 1-D periodic distribution of stacked thin layers of SiO<sub>2</sub> and Si<sub>3</sub>N<sub>4</sub> with different refractive indices forming distributed Bragg reflectors (DBRs). The defect is formed by a cavity layer with a thickness larger than that of the distributed Bragg reflector layers. The resulting resonant peak in the transmission can be chosen to the wavelength where the dye emission is strong and well correlated to the quantity to be sensed. Selection of the number of layers stacked and their thicknesses allows a suitable Q-factor to be achieved.

The dye molecules selected for the dye thin-films in this work are Perylene (PE) for NO<sub>2</sub> detection and Hydroxyflavone (3-HF) for UV detection. The excitation wavelength of PE is between 400 and 480 nm, resulting in a broad emission with maximums at approximately 490 and 510 nm. The excitation wavelength of (3-HF) is between 300 and 380 nm and the emission wavelength is also around 500 nm. As the thickness of the dye thin-films is in the range of 100 nm, the layers do not lead to interferences in the visible range, resulting in an emitted light spectrum that accurately reflects the light emitted by the dye molecules.

## 2.2. Sensor arrangement for NO<sub>2</sub> detection in polluted air

The sensor for the environmental NO<sub>2</sub> sensor system is designed according to Fig. 1b. The excitation and detection setup is shown in Fig. 2. The portable measurement platform demonstrator incorporates a top-side surface illumination source consisting of a UV LED. The electronic read-out is a 4–20 mA current loop, compatible with industrial control instruments used for tunnel safety management. A filter suppresses excitation wavelengths close to the dye fluorescence emission. To increase the signal to noise ratio, a 9 mm diameter aperture lens with 12 mm focal length is used to focus the excitation light on the

centre of the chip, which contains the sensing dye thin-film. This leaves a shadowed area at the edges where the detection takes place.

### 2.3. Sensor arrangement for UV detection of sunlight

The UV sensor system is designed in accordance with Fig. 1a. To detect UV radiation, the top panel of the platform demonstrator shown in Fig. 2 is replaced by a panel with an aperture and two UV band-pass filters (Edmund #46-048 and Spectrogon SP-0400) above the sensing chip to remove the strong visible components of sunlight. The vertical resonant cavity chip with the dye thin-film is mounted directly under the UV filters and the fluorescence is detected on the backside of the chip.

## 3. Design, fabrication, and packaging of the dye-based sensors

### 3.1. Dye thin-film deposition

The dye thin-films for NO<sub>2</sub> sensing are deposited by a RPAVD deposition of PE dye and Adamantane precursor molecules. This technique allows a high concentration of dye molecules to remain intact within a matrix formed by molecular fragments of the same dye and Adamantane generated by interaction with a remote microwave plasma discharge. A cross-linked organic thin-film results, where the PE dye is homogeneously distributed without forming dye aggregates [5].

The UV-sensing dye thin-films are synthesized from 3-HF and Adamantane by the RPAVD technique. The thin-films show an intense green light emission when excited in the UV A+B region, and they are completely transparent in the visible region [16]. All dye-containing polymer thin-films were deposited at room temperature conditions and at wafer scale, using shadow masking for patterning. More details about the synthesis and optical properties of the sensing dye thin-films can be found in references [3–6,17,18]

### 3.2. Design of the vertical resonant cavities

The characteristic emission wavelengths of the dye thin-films (PE and 3-HF) are around 500 nm, as described in section 2.1. The resonant peak of the vertical resonant cavities must be tuned to permit selective transmission of the emitted light at the correct wavelengths, while the Q-factor of the cavities should be selected to achieve a good compromise between the sensitivity and the specificity of the sensor systems. To achieve this, the optical response was simulated and compared with the luminescence spectra of the dye thin-films. The two vertical resonant cavity types each consist of 18 pairs of oxide-nitride layers (SiO<sub>2</sub> thickness = 100 nm and Si<sub>3</sub>N<sub>4</sub> thickness = 65 nm) on both sides of a Si<sub>3</sub>N<sub>4</sub> defect layer; whose thickness is selected to match the resonant mode of the structure with centre of the emission band of the dye film. The transmission spectra of the structures for UV (a) and NO<sub>2</sub> (b) sensing are shown in Fig. 3 in comparison with the emission spectra of the respective bare luminescent films. In these cases the transmission peak is simply positioned at the peak of the emission spectrum and away from any spurious emission from the excitation source to reflect the amplitude change of the emission. For the Q-value there is a trade-off between signal power and signal purity. Other luminescent films may instead exhibit a wavelength shift in the emission spectrum upon exposure to the measurand. The peak should then be designed to convert this shift into a large change in

amplitude. A set of vertical cavities were fabricated and tested following this design principle. The incorporation of a backside reflector was also implemented as an option for some of the structures.

### 3.3. Fabrication and packaging of the sensor chips

For the applications targeted in the present work, the sensor packaging must fulfil the following requirements: (1) The packaging process must be conducted at near room temperature to avoid damage to the dye thin-films. (2) The package has to be UV-transparent to allow excitation of the dyes. (3) The package for the NO<sub>2</sub> gas sensor application must allow gas diffusion to the dye thin-films. (4) The package for the NO<sub>2</sub> sensor must not have any polymer surfaces exposed to the inside of the package cavity to prevent contamination of the dye thin film or NO<sub>2</sub> scavenging. (5) The dye thin-film surfaces must be protected against dust.

The overall wafer-scale integration and packaging of the sensor chips is outlined in Fig. 4, and the sensor package is schematically shown in Fig. 5a. The sensor package consists of a glass cap with a plastically deformable gold gasket that encloses and seals the cavity. The dye thin-film is located inside the cavity on the device wafer. An epoxy underfill is used to provide a permanent bond between the two substrates. The epoxy shrinks during curing, creating a compressive force on the gold gaskets, thereby completing the seal.

For the NO<sub>2</sub> gas sensors, the glass lid is perforated to enable the analyte gas to access the dye thin-film. In the UV sensor, the glass lid does not contain perforations and thus the cavity is sealed to eliminate any gas interaction. An epoxy underfill surrounds the cavity enclosed by the gold gasket and bonds the two substrates together. This design allows efficient room-temperature bonding and sealing of the cavities while at the same time preventing any epoxy underfill from coming into contact with the dye thin-films. To allow gas sensing in environments with particle contaminations, the package design of the NO<sub>2</sub> sensor comprises a three-stage filter. The first stage is formed by the 0.5 x 1 mm gas inlet perforation of the lid. The small distance between the sensing chip and the glass cap chip, which is defined by the gold gasket height, acts as a 1-dimensional particle filter, which is the second stage. A third filter, consisting of closely spaced gold studs, filters smaller particles. Full 3D simulations conducted using Comsol Multiphysics show that the analyte diffusion into the packaged chip closely follows Fick's first law of diffusion. For the dimensions and specific topology of the sensor chips, this means that the centre of the sensing cavity reaches 90 % of the outside NO<sub>2</sub> concentration in less than 2 s. This is one order of magnitude faster than the expected response time of the dye thin-films [5].

For integration and packaging of the sensors, 500 µm thick and 100 mm diameter borofloat glass-cap substrates were sandblasted (Little Things Factory GmbH, Germany) to form wafer through-holes for the underfill stoppers, and to a depth of 100 µm for the underfill channel structures, as shown in Fig. 4a. A 150 nm thick layer of Ti/Au was evaporated to provide a conductive electroplating base on the wafer surface that contains the channels. To form an electroplating mould a 5 µm thick AZ 9260 photo resist (Clariant) was spray-coated and patterned, as illustrated in Fig. 4b. The mould for the 2 µm

wide gold gaskets and filter studs was then filled by electroplating 99.9 % pure gold (EnthoneMicrofab Au 660). The resist mould and the plating base were finally removed by oxygen plasma and wet etching in KI (aq.) and H<sub>2</sub>O<sub>2</sub>, as shown in Fig. 4c.

The device wafers, (500 µm thick borofloat glass with a diameter of 100 mm) were first cleaned in a boiling piranha solution and rinsed in deionized water. The Fabry-Perot resonator consisting of a multilayer silicon oxide and nitride thin-film stack was deposited using plasma enhanced CVD in an Oxford Plasmalab 80+ reactor (Fig. 4d). The entire deposition process was completed in one vacuum cycle at a chuck temperature of 300 °C. To avoid wafer bending due to the thermal expansion mismatch of silicon dioxide and the glass substrate, a SiO<sub>2</sub> layer with the same thickness as the total thickness of the front side stack was deposited on the backside of the glass wafer, as schematically depicted in Fig. 4d. For patterning the subsequently deposited dye thin-film a 25 µm thick polyimide adhesive tape that had been patterned in a cutting plotter was attached to the wafer, as shown in Fig. 4e. As indicated in Fig. 4f, the UV or NO<sub>2</sub> sensing dye thin-films were deposited directly onto the wafers using room-temperature remote plasma deposition. The targeted thickness of the resulting dye layers was 100 nm, which was controlled using a quartz crystal monitor placed in the deposition chamber [3,4,18].

After completing the fabrication of the device and the cap wafers, the wafers were manually aligned under a stereo microscope, according to the layout in Fig. 5b allowing access to the epoxy underfill reservoir after the wafer stack was clamped together. The stack was mounted in a Süss Microtec CB8 wafer bonder which applied a tool force to the wafer stack to compress the gold gaskets, as depicted in Fig. 4g. With the wafers still under tool pressure, 3 ml of low viscous epoxy underfill (Epotek 301, Epoxy Technology) was dispensed in the reservoir. The epoxy was cured for 16 hours at room temperature. A microfluidic network was implemented [12,19] to increase the underfill rate and to achieve a complete coverage of the low viscosity underfill epoxy over the entire wafer with a single injection point. This underfill process was designed to occur in two phases. First, a network of 100 µm high microfluidic channels was filled by capillary forces. As shown in Fig. 5b, this network is connected to a single reservoir and surrounds all regions of the wafer covered with the dye thin-films. Simultaneously, the gap between the two wafers, which is on the order of 3 µm, defines the second phase of capillary driven filling, as shown in Fig. 5c. The epoxy spreads from the channels towards the wafer gap, stopping on the through-etched glass sections, which act as fluidic barriers. These through-etched sections also allow air to escape, facilitating a void-free underfill process. After this second and slower filling phase is complete, all the chips are completely bonded and sealed at wafer-scale. Once the sensor packaging is complete, a reflective layer of 50 nm aluminium can optionally be sputtered on the backside of the bonded device wafer. The sensors were finally diced upside down using a wafer saw. Fig. 6 shows a picture with a finalized UV sensor chip (a) and a finalized NO<sub>2</sub> sensor chip (b) after dicing. At this point it is important to stress that all the different fabrication stages are carried out at wafer level allowing for high-volume manufacturing of inexpensive and even disposable photonic sensor chips.



## 4. Experiments and characterization of the dye-based sensor systems

### 4.1. Characterization of the dye-based sensors and coupling of the luminescence signal

The photonic properties of the vertical resonant cavities were adapted to the luminescent characteristics of the two types of dye sensor films. Thus, by combining a specific sensing layer with the corresponding photonic structure, we fabricated luminescent photonic chips with well resolved sensing signals bearing selective information of different analytes. Fig. 7 a and c compares the emission spectra of reference dye thin-films, deposited on fused silica, with the luminescent output signal of the sensor chips detected through the vertical resonant cavities as shown in Fig. 1a. The graphs show that in the vertical configuration (Fig. 7 a and c) the broad emission band of the dye thin-film is converted into narrow peaks at the resonant modes of the vertical resonant cavity. With this approach, a rather monochromatic (FWHM < 5 nm) luminescent signal is obtained which can be more easily handled in the detection system. This also allows the development of multi-analyte sensing platforms by implementing different photonic chips in a vertical configuration even in the case of fluorescent probes with overlapping fluorescent bands. The narrow sensing signal then simplifies the multiplexing. The inherently filtered lateral emission detected at the chip edges is illustrated in Fig. 7b. This graph shows that the analysed signal corresponds to the out-of-normal fluorescence emission modulated by the photonic structure and laterally guided through the wave-guiding glass substrate. Since the excitation beam impinges normal to the surface, this detection configuration filters the excitation beam and improves the signal to noise ratio. At the same time however, the filtering effect of the photonic structure is modified by the off-normal propagation of the fluorescence light.

### 4.2. Measurement results from the dye-based sensor systems

NO<sub>2</sub> and UV detection experiments were carried out both in the laboratory and in real-world scenarios. For the latter, the packaged sensor chips were used together with the measurement platforms described in sections 2.2 and 2.3. The sensors were evaluated for NO<sub>2</sub> detection in road tunnels and for sunlight UVA+B intensity monitoring.

#### 4.2.1 NO<sub>2</sub> gas detection in polluted air

Experiments were carried out with bare PE dye thin-films to qualitatively assess the evolution of the fluorescence properties upon exposing them to NO<sub>2</sub> concentrations in a road traffic tunnel. For these assessments, several PE thin-films were placed in perforated metallic boxes and exposed to the environment in the road tunnel for a time range between one and seven days. All samples had identical luminescent properties before the exposure to the tunnel environment. Fig. 8 compares the emission spectra of the exposed samples with that of a reference sample stored in the laboratory under NO<sub>2</sub>-free conditions. The results clearly show the gradual quenching of the fluorescence emissions with prolonged exposure to the polluted environment. These results are in line with previous studies showing that this type of PE thin-films act as accumulative sensors during NO<sub>2</sub> detection [4,5]. The effect of the photonic structure is in this case just to pick out the intensity at 490 nm where the response is highest and to create a rather monochromatic signal. For other fluorescent films, the sensing response is more complicated. The transmission peak must then be carefully chosen.

In order to test the functionality of the NO<sub>2</sub> sensor in the portable measurement platform, a set of experiments were carried out in the laboratory. Fig. 9a shows the results of one of these experiments, corresponding to the detection of 10 ppm NO<sub>2</sub> in air. The relatively high concentration was chosen to speed up the characterization time in the experiments. The plot clearly shows that the output signal progressively decreases with the exposure time, which is due to the quenching of the fluorescence emission of the active layer by reaction with the NO<sub>2</sub>. This type of integral curve can be used to derive differential response curves to estimate the actual average NO<sub>2</sub> concentration during defined periods of time.

The NO<sub>2</sub> gas sensing system was finally tested in a road tunnel in Valencia, Spain. The measurements were carried out after calibrating the measurement system with the reference data acquired under controlled conditions in the laboratory. The measurement platform demonstrator, containing the packaged sensor chip, was placed next to an existing commercial NO<sub>2</sub> sensor (Model DF-9200 from MSA) for these experiments. Although the comparative study presented here corresponds to periods of only 2–3 hours, the measurements are consistent with the data registered in a longer experiment lasting 30 days. Fig. 9b shows the measurement data of the dye-based photonic sensor and the existing commercial sensor during rush hours, when the NO<sub>2</sub> concentration reaches maximum values. The measurement data from the photonic platform demonstrator is reasonably stable and in line with the data from the commercial sensor. Agreement between the demonstrator and commercial sensor readings is also observed for low NO<sub>2</sub> concentrations shown in Fig. 9c, thus indicating that the system is sufficiently sensitive for these low analyte levels. The response of both detectors to a dynamic NO<sub>2</sub> signal was examined by placing them in a scenario of increasing traffic. Fig. 9d shows the data registered early in the morning just before rush hour, when the NO<sub>2</sub> concentration increases from 1.5 ppm to 2 ppm. From this figure it is apparent that the concentration values provided by the photonic dye-based sensor gradually increase, as do the registered concentrations of the commercial sensor and that the photonic system has a similar reaction time. Despite the discrepancies observed in the absolute values, the almost parallel responses of our prototype and the commercial device validate the detection principle proposed in the present work.

#### 4.2.2. Sunlight UV detection

Previous research showed that the 3-HF thin-films emit an intense green luminescence when exposed to UV A+B radiation. The emission intensity is proportional to the UV intensity [16–18]. Thus, this emission can be used to determine the level of UV light irradiating a sample. The UV measurement platform was used to measure UV sun intensity over several time periods. As an example, Fig. 10 shows the output signal recorded on the 25<sup>th</sup> of June 2010 in Mons, Belgium. For practical reasons at the time of test, an unpackaged sensor chip was used in this test. However, using a fully packaged chip would not have altered the result in any significant way. For comparison, the UV index values recorded simultaneously by a meteorology station in Soumagne, around 120 km east of Mons [20] is also shown. Note that both data sets depict a similar overall evolution during the 6 hour measurement period, except for some variations due to clouds. The comparable evolution of the two measurements sustains that the room temperature reversible

fluorescence detection of UV light based on the presented measurement principle is reliable, and can be used for monitoring of UV light under real-world conditions.

## 5. Conclusions

In this paper we report on a dye-based photonic sensor platform for UV and NO<sub>2</sub> sensing. For the first time, fully integrated sensing systems based on plasma deposited fluorescent organic nanocomposite thin-films are demonstrated. The fluorescent signal of the dye thin-films responds to changes in the environment and is selectively filtered by a Fabry-Perot resonant cavity photonic structure, onto which the dye thin-film is deposited. The photonic chip thus combines a sensing element and a photonic transducer tuned to the sensing signal in a single package formed at wafer scale.

The sensor systems were evaluated in real-world scenarios in a road tunnel for NO<sub>2</sub> detection and in an open environment for UV detection. The results confirm the suitability of the developed technology for environmental monitoring of different variables. The spectral peaks of the photonic structures are very sensitive to small changes in the wavelength spectral response and intensity of the dye emissions. Thus, the technology is generic and can be expanded to other applications by utilizing different types of thin-films.

The fact that the sensing principle is completely optical and is performed at ambient temperature also allows fibre optical interrogation which brings further advantages, e.g. for use in potentially explosive environments.

The sensing element can be further reduced in size. With the wafer-scale fabrication process employed, this leads to a reduction of the fabrication cost that would potentially allow the use of disposable sensing elements for some applications.

## 6. Acknowledgements

The authors thank the EU (Phodye Strep Project 033793 and ERC Starting Grant M&M's 277879), and the Spanish Ministry of Economy and Competitiveness (MAT-2010-21228) and Junta de Andalucía (P09-TEP-5283) for financial support.

## 7. References

- [1] J. Dakin, B. Culshaw, *Optical Fiber Sensors Volume IV: Applications, Analysis, and Future Trends*, Artech House, Boston, London, 1997.
- [2] S.J. Mihailov, *Fiber Bragg Grating Sensors for Harsh Environments*, *Sensors*. 12 (2012) 1898–1918. doi:10.3390/s120201898.
- [3] A. Barranco, P. Groening, *Fluorescent Plasma Nanocomposite Thin Films Containing Nonaggregated Rhodamine 6G Laser Dye Molecules*, *Langmuir*. 22 (2006) 6719–6722. doi:10.1021/la053304d.
- [4] I. Blaszczyk-Lezak, F.J. Aparicio, A. Borrás, A. Barranco, A. Álvarez-Herrero, M. Fernández-Rodríguez, et al., *Optically Active Luminescent Perylene Thin Films Deposited by Plasma Polymerization*, *J. Phys. Chem. C*. 113 (2009) 431–438. doi:10.1021/jp807634j.
- [5] F.J. Aparicio, I. Blaszczyk-Lezak, J.R. Sánchez-Valencia, M. Alcaire, J.C. González, C. Serra, et al., *Plasma Deposition of Perylene–Adamantane Nanocomposite Thin Films for NO<sub>2</sub> Room-Temperature Optical Sensing*, *J. Phys. Chem. C*. 116 (2012) 8731–8740. doi:10.1021/jp209272s.
- [6] F.J. Aparicio, M. Holgado, A. Borrás, I. Blaszczyk-Lezak, A. Griol, C.A. Barrios, et al., *Transparent Nanometric Organic Luminescent Films as UV-Active Components in Photonic Structures*, *Adv. Mater.* 23 (2011) 761–765. doi:10.1002/adma.201003088.
- [7] K. Najafi, *Micropackaging Technologies for Integrated Microsystems: Applications to MEMS and MOEMS*, in: *SPIE Proc, The International Society for Optical Engineering*, 2003: pp. 1–19. doi:10.1117/12.484953.
- [8] F. Niklaus, G. Stemme, J.-Q. Lu, R.J. Gutmann, *Adhesive wafer bonding*, *J. Appl. Phys.* 99 (2006) 031101. doi:10.1063/1.2168512.
- [9] F. Niklaus, H. Andersson, P. Enoksson, G. Stemme, *Low temperature full wafer adhesive bonding of structured wafers*, *Sens. Actuators Phys.* 92 (2001) 235–241. doi:10.1016/S0924-4247(01)00568-4.
- [10] C.-J. Kim, *Microgasketing and adhesive wicking techniques for fabrication of microfluidic devices*, in: *SPIE Proc*, 1998: pp. 286–291. doi:10.1117/12.322072.
- [11] A. Decharat, J. Yu, M. Boers, G. Stemme, F. Niklaus, *Room-Temperature Sealing of Microcavities by Cold Metal Welding*, *J. Microelectromechanical Syst.* 18 (2009) 1318–1325. doi:10.1109/JMEMS.2009.2030956.
- [12] M.A. Lapisa, F. Niklaus, G. Stemme, *Room-temperature wafer-level hermetic sealing for liquid reservoirs by gold ring embossing*, in: *Solid-State Sens. Actuators Microsyst. Conf. 2009 TRANSDUCERS 2009 Int.*, 2009: pp. 833–836. doi:10.1109/SENSOR.2009.5285763.
- [13] S.-H. Lee, J. Chae, N. Yazdi, K. Najafi, *Micro-Brush Press-On Contact: A New Technique for Room Temperature Electrical and Mechanical Attachment*, in: *19th IEEE Int. Conf. Micro Electro Mech. Syst. 2006 MEMS 2006 Istanb.*, 2006: pp. 342–345. doi:10.1109/MEMSYS.2006.1627806.
- [14] C. Huyghebaert, J. Van Olmen, Y. Civale, A. Phommahaxay, A. Jourdain, S. Sood, et al., *Cu to Cu interconnect using 3D-TSV and wafer to wafer thermocompression bonding*, in: *Interconnect Technol. Conf. IITC 2010 Int.*, 2010: pp. 1–3. doi:10.1109/IITC.2010.5510444.
- [15] M. Lapisa, M. Antelius, A. Tocchio, H. Sohlström, G. Stemme, F. Niklaus, *Wafer-level capping and sealing of heat sensitive substances and liquids with gold gaskets*, *Sens. Actuators Phys.* 201 (2013) 154–163. doi:10.1016/j.sna.2013.07.007.
- [16] F.J. Aparicio, M. Alcaire, A. Borrás, J.C. Gonzalez, F. López-Arbeloa, I. Blaszczyk-Lezak, et al., *Luminescent 3-hydroxyflavone nanocomposites with a tuneable refractive index for photonics and UV detection by plasma assisted vacuum deposition*, *J. Mater. Chem. C*. 2 (2014) 6561–6573. doi:10.1039/C4TC00294F.

- [17] F.J. Aparicio, G. Lozano, I. Blaszczyk-Lezak, Á. Barranco, H. Míguez, Conformal Growth of Organic Luminescent Planar Defects within Artificial Opals, *Chem. Mater.* 22 (2010) 379–385. doi:10.1021/cm902819x.
- [18] A. Barranco, F. Aparicio, A. Yanguas-Gil, P. Groening, J. Cotrino, A.R. González-Elipe, Optically Active Thin Films Deposited by Plasma Polymerization of Dye Molecules, *Chem. Vap. Depos.* 13 (2007) 319–325. doi:10.1002/cvde.200606552.
- [19] M.K. Schwiebert, W.H. Leong, Underfill flow as viscous flow between parallel plates driven by capillary action, *IEEE Trans. Compon. Packag. Manuf. Technol. Part C.* 19 (1996) 133–137. doi:10.1109/3476.507149.
- [20] Données météo de Soumagne (province de Liège), (n.d).  
<http://phitofa.be/meteo.html>.

## Author biographies

### Francisco J. Aparicio

Dr. Francisco J. Aparicio received the PhD Degree from the University of Seville (2011). Afterwards he realized a postdoctoral stay at the University of Trento (Italy) and the University of Mons (Belgium). At the present he is a postdoctoral researcher at the Institute of Materials Science of Seville (CSIC-US). His current research is focused in functional organic thin films by plasma deposition techniques.

### María Alcaire

(Biography not available at the time of submission)

### Agustín R. González-Elipe

Prof. Agustín R. González-Elipe received the PhD degree in Chemistry at the University Complutense of Madrid in 1979 and worked in different laboratories in Paris (Université Pierre et Marie Curie) and Munich (Institut für Physikalische Chemie). He was director of the Institute of Materials Science of Seville and responsible scientist for the Materials Science area of the National Research Council of Spain (CSIC) (1998-2005). At present he leads the Nanotechnology on Surfaces laboratory of the Institute of Materials Science of Seville, joined centre between CSIC and the University of Seville. His present research interests fall within the fields of thin films, plasma technologies and functional materials, these latter mainly in relation with sensor, wetting and photovoltaic applications.

### Angel Barranco

Angel Barranco (MSc Degree in Physical-Chemistry (University of Granada (1995)), PhD Degree in Chemistry (University of Seville (2002)) is Tenured Scientist at the National Research Council of Spain (Materials Science Institute of Seville CSIC-University of Seville) after several postdoctoral stays in France (CNRS) and Switzerland (EMPA-ETH). He was the coordinator of an European Project (Phodye STREP Project ref. 033793) involving eight different academic and industrial partners from four different European countries that aimed the development of the photonic sensing chip technology resumed in this work.

### Miguel Holgado

Dr. Miguel Holgado received the Bachelor's and Master's degree in Electrical Engineering from Technical University of Madrid (UPM) (1996), and Doctoral degree (Ph.D.) at the Institute of Material Science belonging to the Spanish National Research Council CSIC (2000). He is currently group leader of the Optics, Photonics and Biophotonics Technology Lab. at the Center for Biomedical Technology CTB-UPM, and associate professor at the Applied Physics and Material Engineering Department of ETSII (UPM). He worked as R&D engineer at Laser Section of TPYCEA at the Spanish Ministry of Defense and responsible for RAMAN spectroscopy service Lab at ICM-SEV-CSIC. He was process engineer at Lucent Technologies Microelectronics during 4 years, Spanish representative in the 5th and 6th European R&D Framework Programme, Sub-director of RTD projects at Nanophotonics Technology Center and Head of European Communities Unit at CSIC. He have led and participated in 11 European and in 10 National research projects as well as other R&D initiatives. He is author/co-author of more than 40 scientific publications, which have been cited more than 1000 times, and more than 68 communications to congresses. I am also the inventor of 5 patents applications. In

addition, I am also founder of BIOD S.L. focusing on the development and the commercialization of biomedical optical devices.

### **Rafael Casquel**

Rafael Casquel holds PhD degree from the Universidad Politécnica de Madrid (UPM) in 2013, Ingeniero Industrial (2004) degree from the Universidad Politécnica de Valencia, Valencia, Spain. He moved in 2006 to continue with his thesis to the Laser Centre at the Universidad Politécnica de Madrid (UPM), where has remained working in the field of micro and nano optical biosensors, covering from the conception of the sensor, and its theoretical response, until its fabrication and biomolecular response, besides of developing applications of laser-based techniques to photonic chips developing and characterization. At the present moment he is associate professor in the Applied Physics and Material Science department at the Escuela Técnica Superior de Ingenieros Industriales Technical School belonging to the UPM

### **Francisco J. Sanza**

Francisco J. Sanza received Ph.D. Degree from Universidad Politécnica de Madrid (2015), IT Engineer degree in 2008 (Universidad de Navarra, Spain), a M.Sc. in Photonics in 2009 (Universidad Autónoma de Madrid) and a M.Eng. in Laser Technology in 2011 (Universidad Politécnica de Madrid). He is currently senior Researcher at Center for Biomedical Technology belonging to the Universidad Politécnica de Madrid since 2015. His research is focused on micro and nano-fabrication and characterization of optical sensors and biosensors.

### **Amadeu Griol**

Amadeu Griol was born in Valencia, Spain in 1973. He received the telecommunication engineer and Ph.D. degrees from the Universitat Politècnica de València in 1998 and 2003, respectively. His research interests include fabrication, modeling and characterization of electrical and optical devices, especially microwave microstrip filters with harmonic suppression techniques and also Photonic Integrated Circuits and nanophotonics devices. Currently, he is working in the fabrication of optical micro and nanodevices by using electron beam lithography. He authored and coauthored more than 35 papers in international journals and more than 85 contributions to international conferences.)

### **Damien Bernier**

Damien Bernier obtained his PhD degree in 2008 after three years of research activity in silicon on insulator (SOI) nanophotonics at Paris-Sud Institute of Fundamental Electronics (IEF). He is currently working at Multitel a.s.b.l. as a research and development engineer for the Biophotonics group

### **Fabian Dortu**

Dr. Ir. Fabian Dortu received his engineer degree in applied physics from the University of Liège (Belgium) in 2001, and a specialized master degree in materials for microelectronics at the University of Leuven (KUL) in 2002. In 2009, he obtained his PhD at the KUL in collaboration with IMEC on the development of optical methods for the characterization of ultra-shallow junctions in semiconductors. In 2008, he joined the Applied Photonics department of Multitel (Research Institute, Mons Belgium), where he specialised on biophotonics applications. Since 2010 he is leading the Biophotonics group of Multitel.

### **Santiago Cáceres**

Santiago Cáceres (PMP) is Electronic Engineer – communications networking specialization – from the Polytechnic University of Valencia (Spain). He has worked in the past in LE-Technichs (Slovenia), the Technical University of Prague (Czech Republic) and in Generalitat Valenciana (the public administration of the region of Valencia, Spain). He has been involved for more than nine years as senior project manager and business development at the Technology Department of ETRA I+D mainly in the areas of ICT and Security.

### **Mikael Antelius**

Mikael Antelius received the M.Sc. degree in chemical engineering from Uppsala University, Sweden in 2007 and the PhD degree at the department of Micro- and Nanosystems, KTH Royal Institute of Technology, Stockholm, Sweden in 2013. His research interests included silicon photonics and wafer-level vacuum and liquid packaging, particularly with regards to gas sensors. He is currently at APR Technologies.

### **Martin Lapisa**

(Biography not available at the time of submission)

### **Hans Sohlström**

Hans Sohlström received the M. Sc. degree in electrical engineering from KTH Royal Institute of Technology, Stockholm, Sweden, in 1978 and a Ph.D. degree with a thesis about fibre optical magnetic field sensors based on YIG thin films, in 1993. He is now associate professor at the Micro and nanosystems department at the KTH School of Electrical engineering, where he is leading research in micro-optics. He is also responsible for courses in measurement technology.

### **Frank Niklaus**

Frank Niklaus received the Dipl.Ing. degree in mechanical engineering from the Technical University of Munich, Germany and the Ph.D. degree in MEMS from KTH Royal Institute of Technology, Stockholm, Sweden, in 1998 and 2002, respectively. Currently he is a Professor at the Department of Micro and Nanosystems in the School of Electrical Engineering at KTH Royal Institute of Technology, where he is leading research in the area of micro- and nanofabrication.



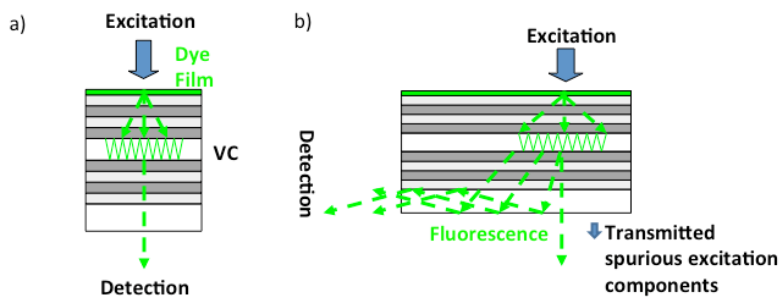


Fig. 1. The principle for the dye-based sensors: a) In UV detection, the detector is behind the chip, b) For  $\text{NO}_2$  sensing, the dye thin-film is supported on the VC and the luminescence is detected at the edge of the chip. The substrate is then used as waveguide for the fluorescence signal. The dashed green lines indicate the fluorescent response (i.e. the sensing signal) whereas the solid blue arrows correspond to the excitation beam.

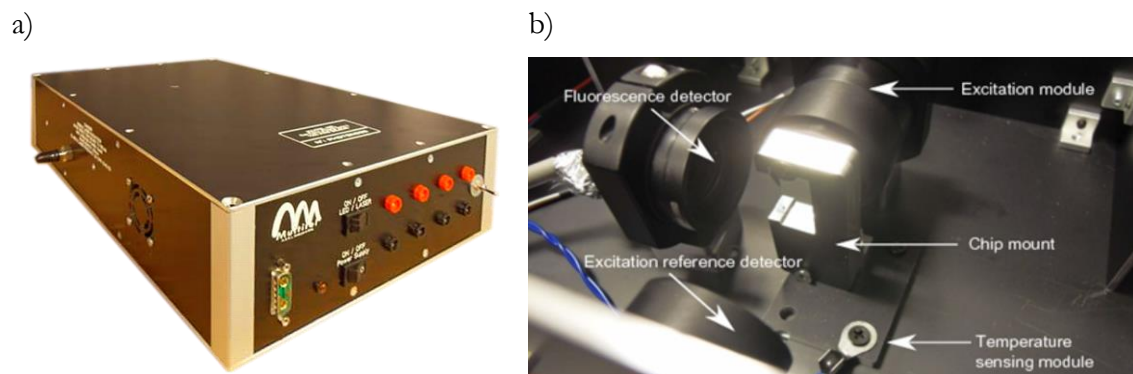


Fig. 2. a) Measurement platform demonstrator for  $\text{NO}_2$  detection showing the gas inlet at the left side panel and various signal outputs (including 4-20 mA) on the front panel. b) Optical setup inside the platform demonstrator.

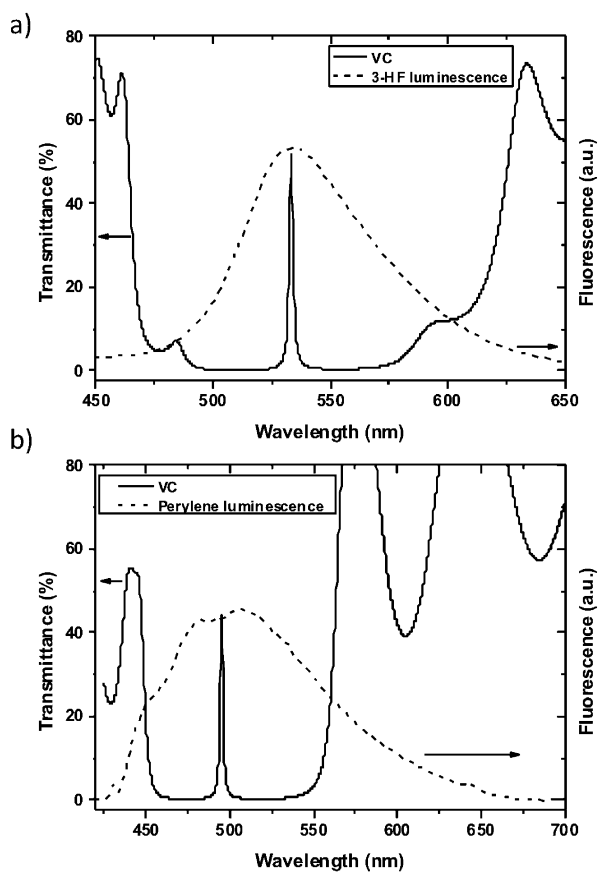


Fig. 3. Measured transmission spectra of vertical resonant cavities (VCs) designed for a) UV sensing and b) NO<sub>2</sub> sensing. The fluorescence spectra of the dye thin-films are included in the figures for comparison.

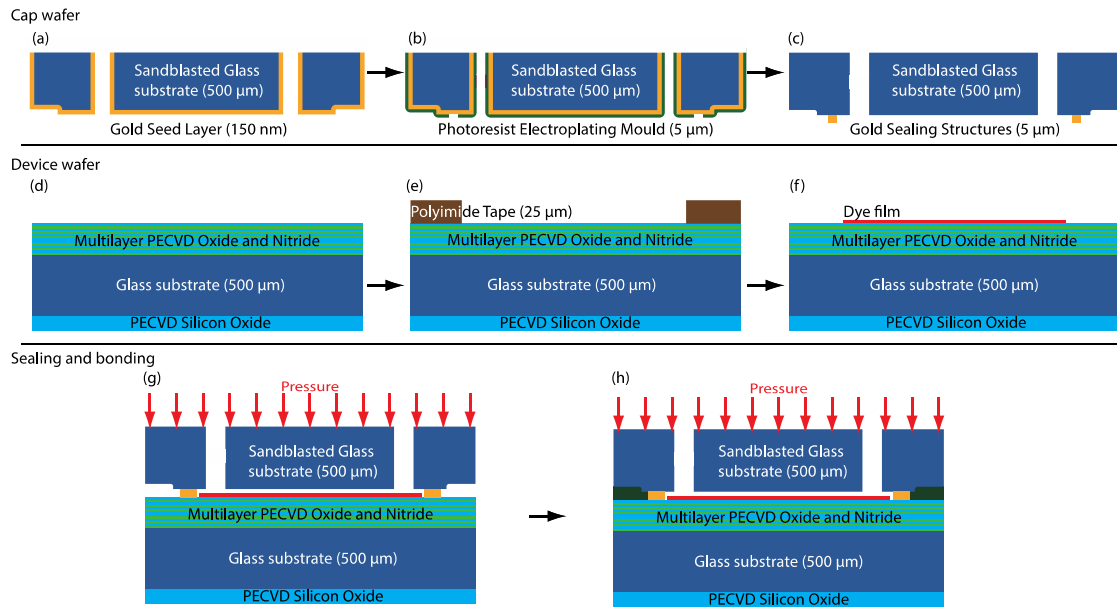


Fig. 4. Outline of the integration and packaging process: The cap wafer (a) to (c) and the device wafer (d) to (f) are processed separately and thereafter aligned, sealed by compression (g) and bonded using an underfill epoxy (h).

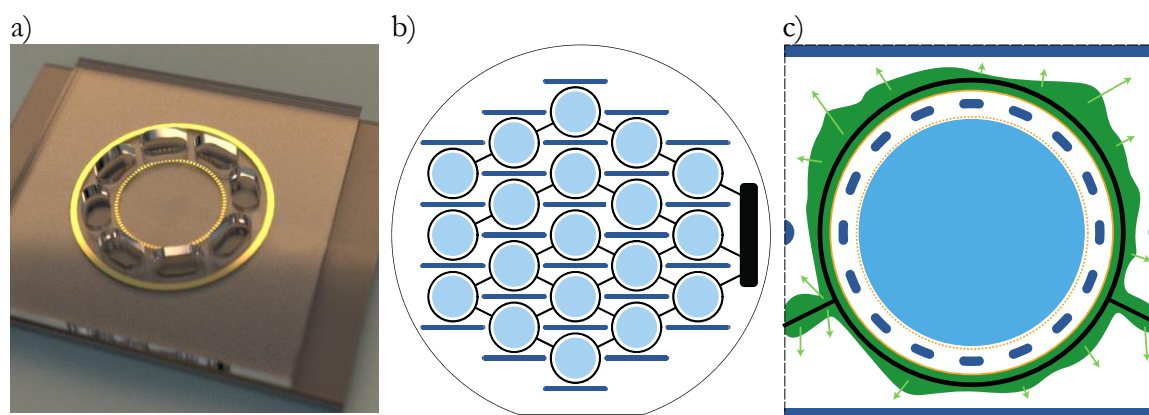


Fig. 5. (a) Computer generated illustration of the package with holes for the  $\text{NO}_2$  sensor chip. The package consists of two glass pieces bonded together with epoxy, which is separated from the cavity by gold gaskets. (b) Layout for the distribution channels (black) for the epoxy underfill on the wafer. Through holes in dark blue (dark gray in print) for the filling process, and dye material in light blue (light gray in print). (c) Close-up of a chip, illustrating that the epoxy underfill (green) is first distributed in the channel (black) and then onto the chip. The gold gasket (orange), the optional gold stud filter (dashed orange) and the cavity ventilation are also visible.

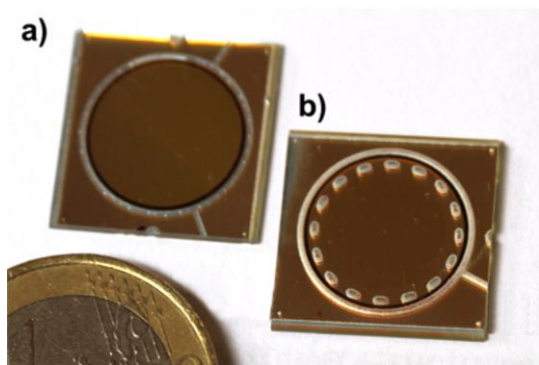


Fig. 6. Packaged devices after wafer scale fabrication and dicing: (a) UV and (b) NO<sub>2</sub> sensing chips.

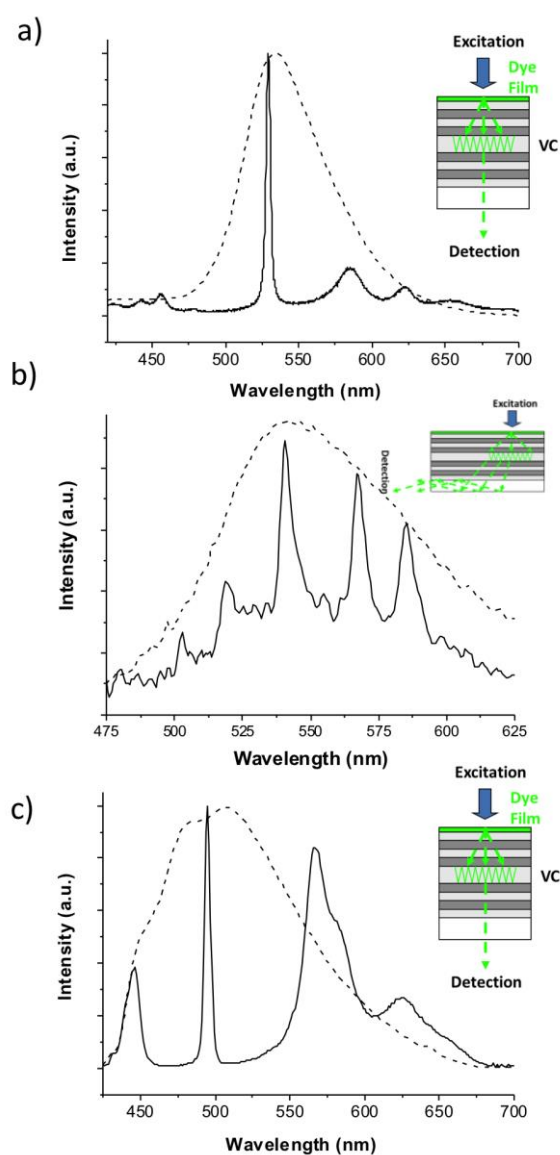


Fig. 7. Luminescent responses of the dye thin-films deposited on the vertical resonant cavity structures. The reference emission spectra of the corresponding luminescent thin-films deposited on glass are included in the figures. These measurements were carried out as indicated in the insets: (a) Emission spectra acquired at the backside of the photonic substrates of a 3-HF thin-film. (b) Lateral emission at the chip edge of the 3-HF thin-film. (c) Emission spectra through the photonic structure of the NO<sub>2</sub> sensing thin-film.

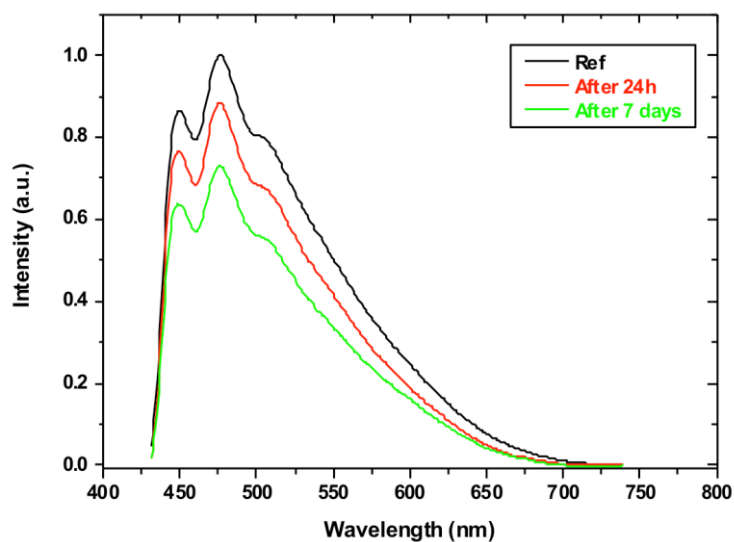


Fig. 8. Emission spectra of the PE thin-films after their exposure between one and seven days to the  $\text{NO}_2$  in the environment of a traffic tunnel with respect to a reference sample stored in the laboratory.



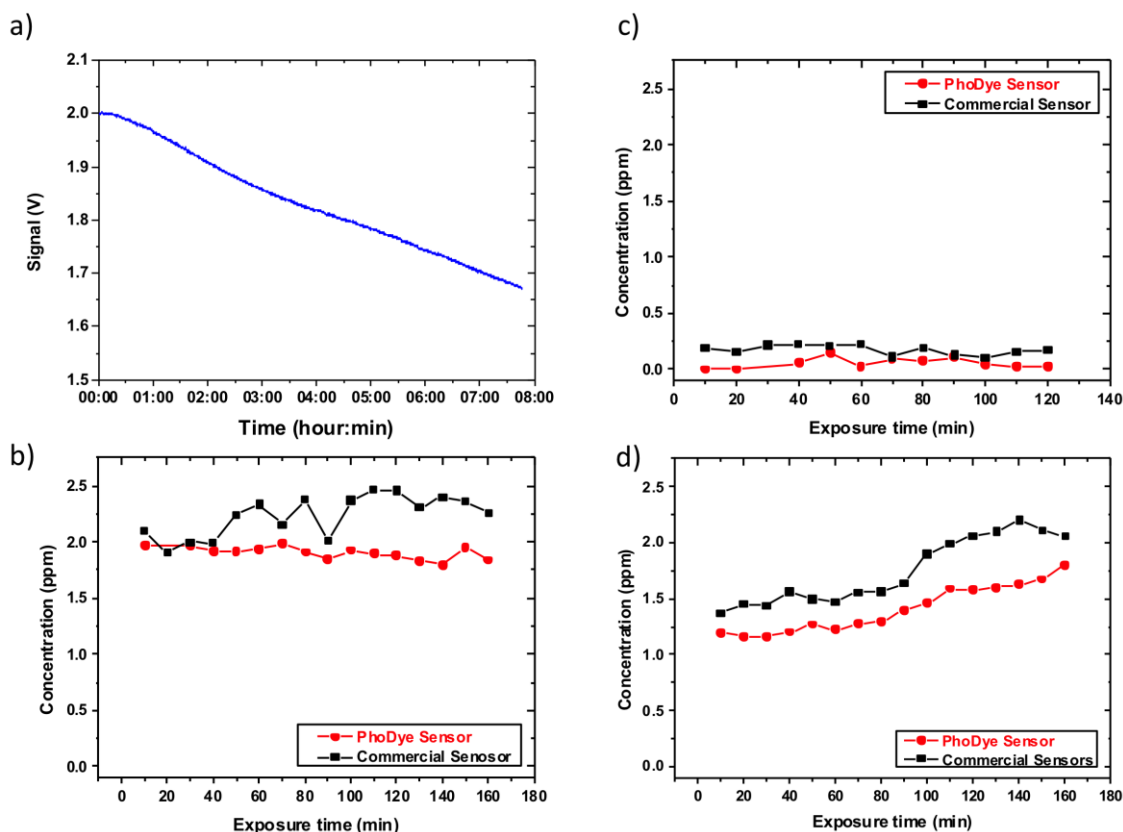


Fig. 9. (a) Measurement of a 10 ppm NO<sub>2</sub> flow in a laboratory experiment. (b)-(d) Measurements of NO<sub>2</sub> concentrations in a traffic tunnel. The graphs compare the measurement data of the dye-based photonic sensor system and a commercial sensor system during time periods with various traffic conditions: (b) High and stable NO<sub>2</sub> concentration. (c) Low and stable NO<sub>2</sub> concentration. (d) Gradually increasing NO<sub>2</sub> concentration.

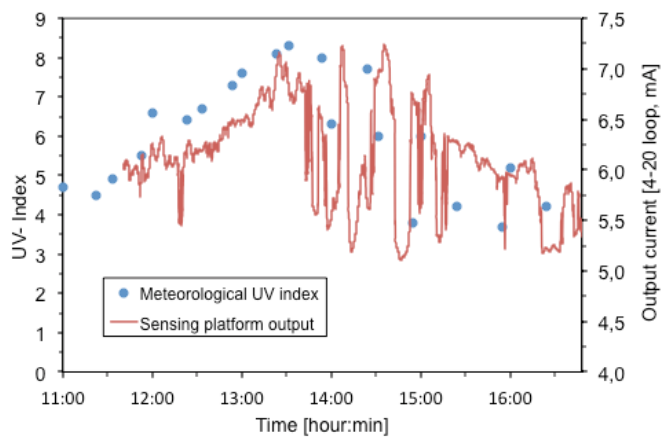


Fig. 10. Output from the measurement platform demonstrator working with the 3-HF sensor chip for UV radiation detection. The blue dots correspond to the sunlight UV index measured by a nearby meteorological station and the red curve corresponds to the output voltage provided by the photonic measurement platform.